

Ten-dimensional neural network emulator for the nonlinear matter power spectrum

Yanhui Yang (杨焱辉)^{1,*}, Simeon Bird^{1,†}, Ming-Feng Ho (何铭峰)^{1,2,3}, and Mahdi Qezlou⁴

¹*Department of Physics & Astronomy, University of California, Riverside, 900 University Ave., Riverside, CA 92521, USA*

²*Department of Physics, University of Michigan, 450 Church St, Ann Arbor, MI 48109, USA*

³*Leinweber Center for Theoretical Physics, 450 Church St, Ann Arbor, MI 48109, USA and*

⁴*The University of Texas at Austin, 2515 Speedway Boulevard, Stop C1400, Austin, TX 78712, USA*

(Dated: July 11, 2025)

We present `GokuNEmu`, a ten-dimensional neural network emulator for the nonlinear matter power spectrum, designed to support next-generation cosmological analyses. Built on the `Goku` N -body simulation suite and the `T2N-MusE` emulation framework, `GokuNEmu` predicts the matter power spectrum with $\sim 0.5\%$ average accuracy for redshifts $0 \leq z \leq 3$ and scales $0.006 \leq k/(h \text{ Mpc}^{-1}) \leq 10$. The emulator models a 10D parameter space that extends beyond Λ CDM to include dynamical dark energy (characterized by w_0 and w_a), massive neutrinos ($\sum m_\nu$), the effective number of neutrinos (N_{eff}), and running of the spectral index (α_s). Its broad parameter coverage, particularly for the extensions, makes it the only matter power spectrum emulator capable of testing recent dynamical dark energy constraints from DESI. In addition, it requires only ~ 2 milliseconds to predict a single cosmology on a laptop, orders of magnitude faster than existing emulators. These features make `GokuNEmu` a uniquely powerful tool for interpreting observational data from upcoming surveys such as LSST, *Euclid*, the Roman Space Telescope, and CSST.

INTRODUCTION

Cosmological surveys [e.g. 1–6] constrain cosmological models motivated by unresolved fundamental physics questions, such as the accelerated expansion of the Universe [7], the nature of dark matter (DM) [8], the sum of the neutrino masses [9], and the parameter tensions found in Λ CDM [e.g. 10–13]. Interpreting these measurements requires an accurate understanding of how the underlying cosmological parameters affect the growth of large-scale structure (LSS) in the Universe. Pre-trained simulation-based cosmological emulators which predict summary statistics are used for this purpose, obviating the need for intensive numerical computation at every likelihood evaluation [e.g. 14–37]. However, none of the existing emulators (except `GokuEmu` [35]) cover a wide enough prior parameter range to match recent dark energy constraints [38–40], nor are they scalable to higher dimensional parameter spaces due to the high cost of running high-fidelity training simulations. Here we present a new emulator, `GokuNEmu`, a highly accurate and computationally efficient neural network model which achieves uniquely broad coverage of parameter and redshift space by using the `Goku` simulations [35].

The `Goku` simulations were the first to expand the parameter space to 10 dimensions, including the 5-parameter base Λ CDM model and several extensions which directly impact the matter power spectrum. These are: dynamical dark energy (characterized by w_0 and w_a), massive neutrinos ($\sum m_\nu$), the effective number of neutrinos (N_{eff}), and running of the spectral index (α_s). The `Goku` suite covers a uniquely wide prior range of dynamical DE parameters, making it the *only* simulation suite to safely cover recent constraints from DESI [38, 39] and DES [40]. `Goku` uses a multifidelity (MF) strategy

[41, 42], where a large number of lower cost simulations explore parameter space and are corrected by a small number of high cost, more accurate, simulations, reducing the total computational cost by 94% [35]. The simulations were used to build a Gaussian process (GP) emulator for the nonlinear matter power spectrum, called `GokuEmu` [35].

We present `GokuNEmu`, a neural network (NN) emulator trained on `Goku` for the nonlinear matter power spectrum using `T2N-MusE`, an MF emulation framework we developed for training highly optimized fully-connected neural networks (FCNNs) [43]. While GP regression has been widely used in cosmological emulation, NNs offer greater efficiency in both training and inference, particularly in high-dimensional parameter spaces and with large datasets. Given that the `Goku` simulations consist of 1128 pairs of low-fidelity (LF) simulations and 36 high-fidelity (HF) simulations,¹ NNs are a more suitable choice in this case.

`T2N-MusE` enables efficient training of `GokuNEmu` on 34 redshift bins between 0 and 3, ensuring more accurate interpolation of the matter power spectrum in redshift space than its predecessor (which included 6 redshifts). It also allows us to cover a broader range of spatial scales, from $0.006h/\text{Mpc}$ to $10h/\text{Mpc}$, by combining two MF models trained on low- and high- k ranges respectively.² Also, `GokuNEmu` achieves a significantly better generalization accuracy and is orders of magnitude more efficient in evaluation time than other emulators. `GokuNEmu` will be especially useful for surveys that measure structures

¹ Existing emulators were typically trained on ~ 100 samples.

² The emulation technique used in `GokuEmu` did not allow covering the full spatial range allowed by the simulations.

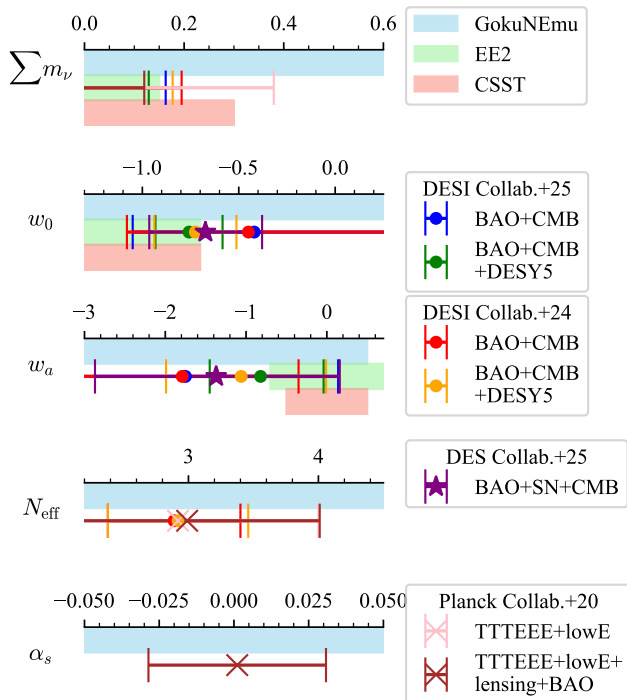


FIG. 1. Prior ranges of the Λ CDM extensions of different emulators and selected cosmological constraints from the literature. The sky blue, light green, and salmon bars represent the prior ranges of GokuNEmu (this work), EuclidEmulator2, and the CSST Emulator, respectively. The constraints are shown with error bars denoting $\pm 3\sigma^a$ uncertainties (though 95% upper limits are shown for $\sum m_\nu$). The constraints are selected from DESI [38, 44], DES [40], and *Planck* [45].

^a Here, σ is defined from the 68% credible interval.

down to nonlinear scales, such as LSST [2], *Euclid* [3], the Roman Space Telescope [4], and CSST [5].

METHODS

This section describes the data and methods used to build the emulator GokuNEmu. We quantify the generalization performance of the emulator using leave-one-out cross-validation (LOOCV). HF samples are iteratively excluded from the training set and used as test points. The leave-one-out (LOO) error is defined as the relative mean absolute error (rMAE) of the emulator prediction with respect to the matter power spectrum measured from the corresponding simulation, denoted as Φ_{rMAE} .

Goku Simulations

We briefly describe the Goku simulations here (for more details, see Ref. [35]). The Goku simulations are a suite of N -body simulations run with the MP-Gadget code [46].

TABLE I. Parameter boxes for Goku-W and Goku-N defined through their lower and upper bounds.

Parameter	min(W)	min(N)	max(N)	max(W)
Ω_m	0.22	0.26	0.35	0.40
Ω_b	0.040	0.045	0.051	0.055
h	0.60	0.64	0.74	0.76
A_s	1.0×10^{-9}	1.7×10^{-9}	2.5×10^{-9}	3.0×10^{-9}
n_s	0.80	0.95	1.00	1.10
w_0	-1.30	-1.30	-0.70	0.25
w_a	-3.0	-1.0	0.5	0.5
$\sum m_\nu$	0.00	0.06 eV	0.15 eV	0.60 eV
N_{eff}	2.2	2.3	3.7	4.5
α_s	-0.05	-0.03	0.03	0.05

Goku's cosmologies are sampled using a Sliced Latin Hypercube Design [47]. An adaptive sampling strategy is used to sample the parameter space, which consists of two Latin hypercubes: a small hypercube with narrow ranges of cosmological parameters, Goku-N, and a large hypercube, Goku-W. Assuming a flat Universe, Goku covers 10 cosmological parameters: the base Λ CDM parameters including the matter density Ω_m , the baryon density Ω_b , the dimensionless Hubble parameter h , the primordial spectral index n_s , and the amplitude of the primordial power spectrum A_s , the parameters for time-dependent DE: w_0 and w_a [48, 49], the sum of the neutrino masses $\sum m_\nu$ [50, 51], the effective number of ultrarelativistic neutrinos N_{eff} [52–54], and the running of the spectral index α_s . The ranges of the parameters are listed in Table I. Fig. 1 shows the prior ranges for Λ CDM extensions in Goku (thus the emulator GokuNEmu) compared to those of other emulators and recent constraints from DESI [38, 44], DES [40], and *Planck* [45]. We observe that many of the constraints on w_0 and w_a are out of the capabilities of the other emulators, while GokuNEmu covers them safely. Also, EE2 struggles to cover some of the upper limits of $\sum m_\nu$, while Goku's prior range is more than sufficient and notably includes the direct neutrino-mass measurement from the KATRIN experiment [55] (which is independent of the cosmological model), $\sum m_\nu < 0.45$ eV (90% confidence level). As for N_{eff} and α_s , GokuNEmu is also able to test the results from *Planck* [45].

The Goku-W (-N) set consists of 564 pairs of LF simulations and 21 (15) HF simulations. Each HF simulation evolves 3000^3 particles within a comoving volume of $(1000 \text{ Mpc}/h)^3$. The LF simulations are divided into two types: L1 and L2. Both L1 and L2 simulations include 750^3 particles, significantly fewer than the HF runs. While L1 simulations share the same box size as the HF simulations, L2 simulations are run in smaller volumes with side lengths of $250 \text{ Mpc}/h$. In this setting, the L1 simulations are used to cover the low- k (large-scale) range, while the L2 simulations are more accurate in the high- k (small-scale) range (see Fig. 7 of Ref. [35]). The LF samples in emulation are responsible for interpolation

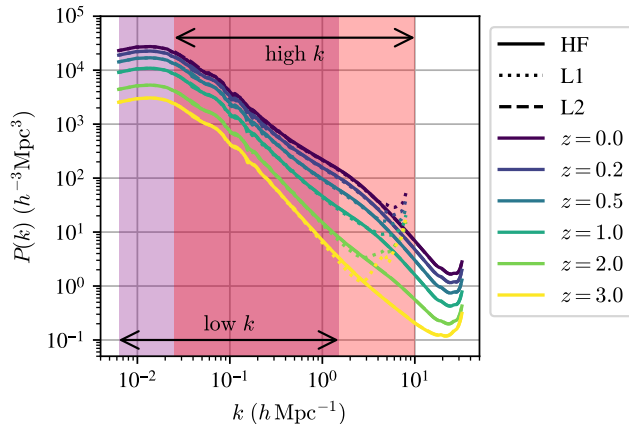


FIG. 2. The matter power spectra measured from the Goku-N-0195 (see Table V of Ref. [35] for the values of the cosmological parameters) simulations at $z = 0, 0.2, 0.5, 1, 2,$ and 3 (color coded). The solid lines represent the HF spectrum, while the dotted and dashed lines represent the L1 and L2 spectra, respectively. The purple and red shaded regions indicate the low- and high- k ranges, respectively.

(exploring the parameter space), while the HF samples are used to correct the bias of the LF samples.

Data and Combination of Emulators

For each of the simulations, in addition to the 6 fixed redshift bins at $z = 0, 0.2, 0.5, 1, 2,$ and 3 , the matter power spectrum was also computed and saved at $\gtrsim 100$ redshifts between $z = 0$ and $z = 3$.³ We interpolate the matter power spectrum at 28 extra z bins within $0 < z < 3$, evenly spaced in $\ln a$ (where a is the scale factor), and combine them with the original 6 redshifts to form a total of 34 redshift bins. We have confirmed that these 34 z bins are sufficient to recover the original output of the simulations, with negligible interpolation error $\lesssim 10^{-3}$.

We build two separate emulators for low and high- k scale ranges. These emulators cover $0.006 < k_{\text{low}}/(h \text{ Mpc}^{-1}) < 1.5$ and $0.025 < k_{\text{high}}/(h \text{ Mpc}^{-1}) < 10$, respectively. As shown in Fig. 2, the L1 simulation matches the HF simulation well at large scales but deviates from it at $k \gtrsim 1.5h/\text{Mpc}$ significantly due to insufficient resolution. The L2 simulation has a maximum box size limiting it to $k > 0.025h/\text{Mpc}$, but is a good approximation to the HF simulation on small scales. We trim the range of data used to train each emulator, as including poorly converged scales can de-

grade the performance of the emulator across the entire spatial range. For the low- k emulator (hereafter, Emu1), the L1 and HF power spectra are truncated at $k_{\text{low,max}} = 1.5h/\text{Mpc}$ before being used for training. For the high- k emulator (hereafter, Emu2), the L2 and HF power spectra are truncated at $k_{\text{high,min}} = 0.025h/\text{Mpc}$ and $k_{\text{high,max}} = 10h/\text{Mpc}$ before serving as training data.

Our low and high- k emulators predict overlapping scales. We blend the two emulators through a smooth ramp function to avoid discontinuities. Specifically, between $k_{\text{min}} = 0.025h/\text{Mpc}$ and $k_{\text{max}} = 1.5h/\text{Mpc}$, the prediction of the final emulator is given by

$$P(k, z) = [1 - w(k)] \cdot P_{\text{Emu1}}(k, z) + w(k) \cdot P_{\text{Emu2}}(k, z), \quad (1)$$

where $w(k)$ is the weight function. We define $w(k)$ as a sigmoid function, i.e.,

$$w(k) = \frac{1}{1 + \exp\left[-s \cdot \frac{k - k_{\text{mid}}}{k_{\text{max}} - k_{\text{min}}}\right]} \quad (2)$$

where $k_{\text{mid}} = (k_{\text{min}} + k_{\text{max}})/2$, and $s = 4$ is a scaling factor that controls the steepness of the transition, chosen to minimize validation error.

Following Ref. [35], we apply a universal pairing-and-fixing [56] correction function to the final emulator output to mitigate cosmic variance.

Emulation with T2N-MusE

The T2N-MusE framework builds highly optimized multi-fidelity emulators based on FCNNs and is fully described in the companion paper [43]. The NNs have a 2-step architecture, in which step 1 is an LF model and step 2 corrects the LF output via learning the mapping between the input (cosmological parameters) and the ratio of the HF output to the LF output. A 2-stage Bayesian optimization process is used to optimize the hyperparameters of the NNs: the number of layers, the number of neurons in each layer, and the strength of L2 regularization (which prevents overfitting). The first stage is a coarse search over a wide range of hyperparameters, while the second stage is a fine search within a smaller space. To train the LF model, a 2-phase training strategy is used. First, multiple random seeds are used to search for a good local minimum which serves as the initial point for the k -fold training and cross-validation. In brief, we use T2N-MusE to build Emu1 and Emu2 separately. For more details of T2N-MusE, we refer the reader to Ref. [43].

RESULTS

Fig. 3 shows the LOOCV results of GokuNEmu in the Goku-W (top) and Goku-N (bottom) parameter boxes. In

³ Redshifts given by particle-mesh steps and comoving distance separations of $80 \text{ Mpc}/h$.

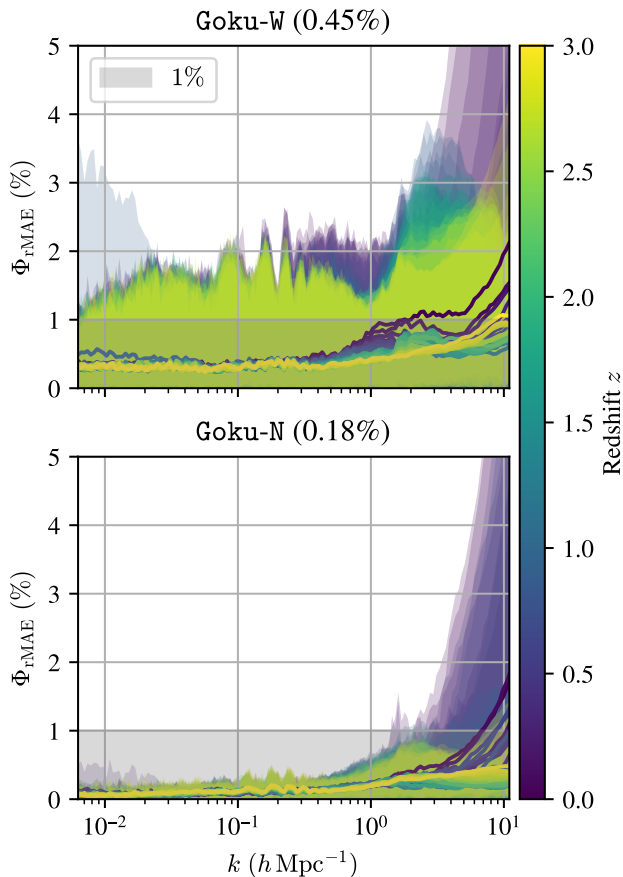


FIG. 3. LOO errors of GokuNEmu in the Goku-W (top) and Goku-N (bottom) parameter spaces. Redshifts are color coded. The solid lines are the error averaged over cosmologies, and the corresponding shaded regions indicate the range of individual cosmologies. The gray-shaded areas mark the region where the error is less than 1%. For each space, the mean error averaged over all the test points, 34 redshifts and 137 k bins is shown in the title of the corresponding panel.

both the wide and narrow ranges, the emulator achieves percent-level accuracy with only mild exceptions at the lowest redshifts and smallest scales. We note that the overall mean error in the wide-prior range Goku-W suite, 0.45%, is substantially lower than its GP-based predecessor GokuEmu’s error of 2.92%, which used the same simulation data, (see Fig. 13 of Ref. [35]). The worst-case error is improved even more significantly. For the Goku-N suite, the mean error is 0.18%, similar to the already small error of GokuEmu (see Fig. 14 of Ref. [35]). However, the error at small scales, especially at $k \gtrsim 2h/\text{Mpc}$ and $z = 0$, is significantly reduced.

We tested the inference speed of GokuNEmu and found that it takes only ~ 2 ms to make a prediction for a single cosmology on a laptop, two orders of magnitude faster than EE2 (~ 300 ms per evaluation) [32] and about 7 times faster than the CSST Emulator (~ 15 ms per evalu-

ation) [33].

With the trained emulator, we perform a simple parameter sensitivity study by varying the parameters of dynamical DE and massive neutrinos, and measuring the change in the matter power spectrum at different redshifts. The reference cosmology is defined as $\theta_{\text{ref}} = (\Omega_m, \Omega_b, h, A_s, n_s, w_0, w_a, \sum m_\nu, N_{\text{eff}}, \alpha_s) = (0.31, 0.048, 0.68, 2.1 \times 10^{-9}, 0.96, -1, 0, 0.06 \text{ eV}, 3.044, 0)$. In addition, we define a cosmology similar to the constraint from DESI BAO+CMB+DESY5 [38] as $\theta_D = (w_0, w_a) = (-0.76, -0.82)$, with other parameters the same as the reference cosmology, and compare the matter power spectrum of θ_D to that of θ_{ref} . Note that the DESI-like cosmology is not a perfect match to DESI, since the values of the other parameters are not guaranteed to be the same, but it is close enough to offer some insight into how a DESI preferred cosmology differs from a Λ CDM counterpart.

In Fig. 4, we show the variation of the matter power spectrum induced by varying the cosmological parameters w_0 , w_a , and $\sum m_\nu$. The first two columns show that the effects of time-dependent DE are more pronounced at lower redshifts, which is expected as the DE density becomes more significant compared to the matter density at lower redshifts. The third column shows that the effect of massive neutrinos is considerable at all redshifts. We see that the k mode most sensitive to the variation of each of the parameters is $\sim 1h/\text{Mpc}$, deep in the non-linear regime, for $z < 1$. While θ_D is far away from the reference cosmology θ_{ref} in the w_0 - w_a plane, the matter power spectrum of θ_D (hereafter, P_D) differs from that of θ_{ref} by only a few percent. This is consistent with expectations, as the equation of state parameter of DE, $w(z)$, evolves from below -1 to above -1 over time (also known as “phantom-crossing”), and the value never deviates too much from -1 at any redshift, with the given w_0 and w_a values.⁴ We see that $P_D(z = 0)$ is consistent with $P_{\text{ref}}(z = 0)$ over large scales but deviates from it at small scales, implying information across scales can help break the degeneracy between the cosmological parameters. Also, we notice that $P_D(z = 1)$ appears very similar to $P_{\text{ref}}^{w_0 = -1.06}(z = 1)$ (the cosmology differs from θ_{ref} only in w_0), while they are different at $z = 0$, indicating that the redshift evolution of the matter power spectrum is useful for breaking degeneracies. Similar findings can also be observed for $P_D^{w_a = -0.04}$ and $P_{\text{ref}}^{w_a = 0.5}$ (see the second column). We note the increase in $P_D(z = 1)$ over $P_{\text{ref}}(z = 1)$ mirrors the increase in the power spectrum for neutrino masses lower than 0.06 eV, the minimum

⁴ In contrast, if we changed the sign of w_a , i.e., $w_a = 0.82$, the value of $w(z)$ would always be above -1 (before $z = 0$), and the matter power spectrum would be significantly different from that of θ_{ref} , even though the distance between the new w_0 - w_a point and θ_{ref} is the same as that of θ_D .

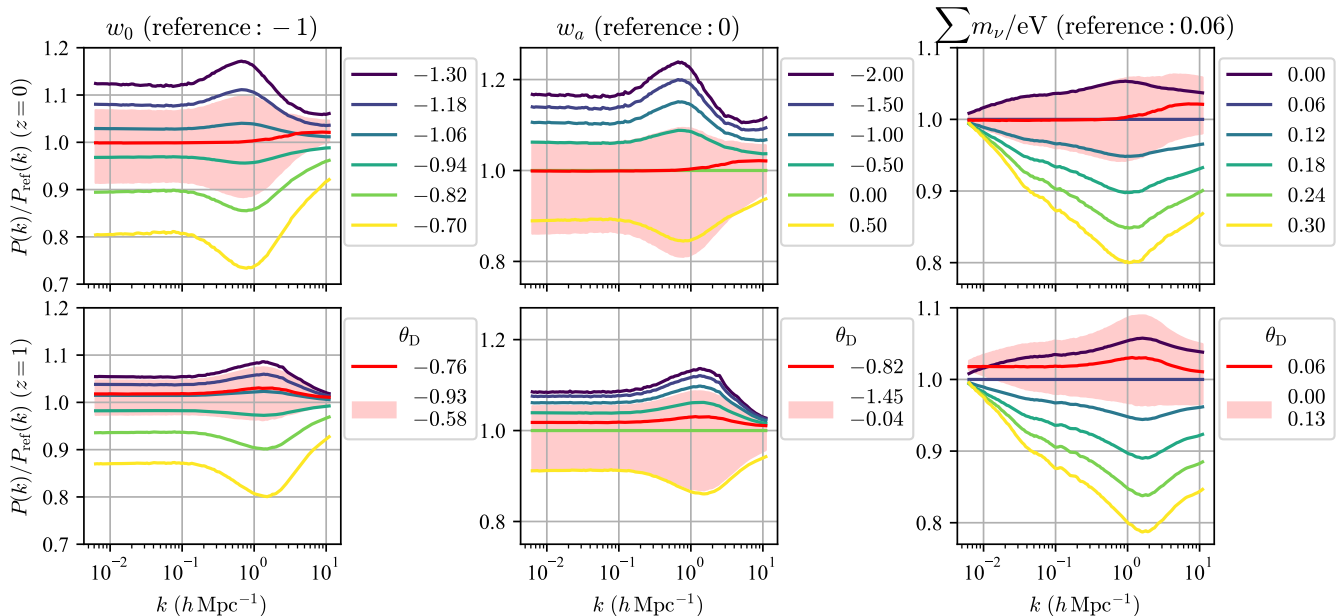


FIG. 4. Variation of the matter power spectrum induced by varying the cosmological parameters w_0 , w_a , and $\sum m_\nu$ at $z = 0$ and 1. The curves are the ratio of the matter power spectrum at the varied parameter value to the spectrum at the reference cosmology (θ_{ref}). The red lines show the ratio of the matter power spectrum of the DESI-like cosmology (θ_{D} , with only w_0 and w_a different from θ_{ref}) to that of θ_{ref} . The shaded regions indicate the corresponding 3σ bounds.

from oscillation experiments. This illustrates the reason for DESI's preference for a low $\sum m_\nu$ in models where w_0, w_a are enforced to be $(-1, 0)$, away from their preferred values [57].

CONCLUSION

We have built the most powerful emulator for the nonlinear matter power spectrum to date, *GokuNEmu*, using the *T2N-MuSE* framework. This emulator covers a 10D cosmological parameter space, including the base flat- Λ CDM parameters, the parameters for time-dependent DE, the sum of neutrino masses, the effective number of ultrarelativistic neutrinos, and the running of the primordial spectral index. It is capable of predicting the matter power spectrum at arbitrary redshifts between 0 and 3 and scales from $0.006h/\text{Mpc}$ to $10h/\text{Mpc}$, with percent-level accuracy (Fig. 3). It is also the fastest emulator for the matter power spectrum, taking only ~ 2 ms to make a prediction for a single cosmology on a usual laptop.

Not only does *GokuNEmu* have an unprecedentedly high-dimensional parameter space, but it also has the widest prior coverage of the extended cosmological parameters. In particular, the prior coverage (Fig. 1) makes it the *only* (besides its predecessor) matter power spectrum emulator that can be used to test recent constraints from DESI [38, 44] and DES [40], for dynamical DE models. In addition, the prior range of the sum of neutrino masses,

$\sum m_\nu/eV \in [0, 0.6]$, covers recent constraints more safely.

GokuNEmu enables the breaking of parameter degeneracies by providing accurate predictions of structure growth across a range of redshifts and spatial scales (Fig. 4). For example, we show an evolving DE model with parameters similar to those derived from DESI. Changes in w_0 and w_a mirror the effect of low $\sum m_\nu < 0.06$ eV. This degeneracy explains how parameter inference under a restricted Λ CDM cosmology, rather than w_0w_a CDM, can drive an apparent preference for unphysically low neutrino masses [57]. The broad parameter coverage of our emulator makes it particularly useful for cosmological analyses in future surveys that can measure cosmic structures with high precision down to nonlinear scales, such as LSST, *Euclid*, the Roman Space Telescope, and CSST. We have made the emulator publicly available at <https://github.com/astro-YYH/GokuNEmu>.

ACKNOWLEDGMENTS

We thank Ye (Issac) Lin for testing the emulator on machines with different architectures (ARM and x86). YY and SB acknowledge funding from NASA ATP 80NSSC22K1897. MFH is supported by the Leinweber Foundation and DOE grant DE-SC0019193. Computing resources were provided by Frontera LRAC AST21005. The authors acknowledge the Frontera and Vista computing projects at the Texas Advanced Computing Cen-

ter (TACC, <http://www.tacc.utexas.edu>) for providing HPC and storage resources that have contributed to the research results reported within this paper. Frontera and Vista are made possible by National Science Foundation award OAC-1818253.

* yyang440@ucr.edu

† sbird@ucr.edu

- [1] DESI Collaboration, A. Aghamousa, and J. Aguilar et al., The DESI Experiment Part I: Science, Targeting, and Survey Design, arXiv e-prints , arXiv:1611.00036 (2016), arXiv:1611.00036 [astro-ph.IM].
- [2] P. A. Abell et al., *LSS Science Book, Version 2.0* (arXiv, 2009) arXiv:0912.0201 [astro-ph.IM].
- [3] R. Laureijs et al., Euclid Definition Study Report, arXiv e-prints , arXiv:1110.3193 (2011), arXiv:1110.3193 [astro-ph.CO].
- [4] R. Akeson et al., The Wide Field Infrared Survey Telescope: 100 Hubbles for the 2020s, arXiv e-prints , arXiv:1902.05569 (2019), arXiv:1902.05569 [astro-ph.IM].
- [5] Y. Gong, X. Liu, Y. Cao, X. Chen, Z. Fan, R. Li, X.-D. Li, Z. Li, X. Zhang, and H. Zhan, Cosmology from the Chinese Space Station Optical Survey (CSS-OS), *Astrophys. J.* **883**, 203 (2019), arXiv:1901.04634 [astro-ph.CO].
- [6] M. Takada, R. S. Ellis, M. Chiba, J. E. Greene, H. Aihara, N. Arimoto, K. Bundy, J. Cohen, O. Doré, G. Graves, J. E. Gunn, T. Heckman, C. M. Hirata, P. Ho, J.-P. Kneib, O. Le Fèvre, L. Lin, S. More, H. Murayama, T. Nagao, M. Ouchi, M. Seiffert, J. D. Silverman, L. Sodr e, D. N. Spergel, M. A. Strauss, H. Sugai, Y. Suto, H. Takami, and R. Wyse, Extragalactic science, cosmology, and Galactic archaeology with the Subaru Prime Focus Spectrograph, *Publications of the Astronomical Society of Japan* **66**, R1 (2014), arXiv:1206.0737 [astro-ph.CO].
- [7] R. R. Caldwell and M. Kamionkowski, The Physics of Cosmic Acceleration, *Annual Review of Nuclear and Particle Science* **59**, 397 (2009), arXiv:0903.0866 [astro-ph.CO].
- [8] J. L. Feng, Dark Matter Candidates from Particle Physics and Methods of Detection, *Annual Review of Astronomy and Astrophysics* **48**, 495 (2010), arXiv:1003.0904 [astro-ph.CO].
- [9] Y. Y. Y. Wong, Neutrino Mass in Cosmology: Status and Prospects, *Annual Review of Nuclear and Particle Science* **61**, 69 (2011), arXiv:1111.1436 [astro-ph.CO].
- [10] A. G. Riess, S. Casertano, W. Yuan, J. B. Bowers, L. Macri, J. C. Zinn, and D. Scolnic, Cosmic Distances Calibrated to 1% Precision with Gaia EDR3 Parallaxes and Hubble Space Telescope Photometry of 75 Milky Way Cepheids Confirm Tension with Λ CDM, *Astrophysical Journal Letters* **908**, L6 (2021), arXiv:2012.08534 [astro-ph.CO].
- [11] A. G. Riess et al., A Comprehensive Measurement of the Local Value of the Hubble Constant with 1 km s⁻¹ Mpc⁻¹ Uncertainty from the Hubble Space Telescope and the SH0ES Team, *Astrophysical Journal Letters* **934**, L7 (2022), arXiv:2112.04510 [astro-ph.CO].
- [12] M. Asgari, C.-A. Lin, B. Joachimi, B. Giblin, C. Heymans, H. Hildebrandt, A. Kannawadi, B. St olzner, T. Tr oster, J. L. van den Busch, A. H. Wright, M. Bilicki, C. Blake, J. de Jong, A. Dvornik, T. Erben, F. Getman, H. Hoekstra, F. K ohlinger, K. Kuijken, L. Miller, M. Radovich, P. Schneider, H. Shan, and E. Valentijn, KiDS-1000 cosmology: Cosmic shear constraints and comparison between two point statistics, *Astronomy & Astrophysics* **645**, A104 (2021), arXiv:2007.15633 [astro-ph.CO].
- [13] DES Collaboration, T. M. C. Abbott, and M. Aguena et al., Dark Energy Survey Year 3 results: Cosmological constraints from galaxy clustering and weak lensing, *Phys. Rev. D* **105**, 023520 (2022), arXiv:2105.13549 [astro-ph.CO].
- [14] K. Heitmann, D. Higdon, M. White, S. Habib, B. J. Williams, E. Lawrence, and C. Wagner, THE COYOTE UNIVERSE. II. COSMOLOGICAL MODELS AND PRECISION EMULATION OF THE NONLINEAR MATTER POWER SPECTRUM, *The Astrophysical Journal* **705**, 156 (2009).
- [15] K. Heitmann, M. White, C. Wagner, S. Habib, and D. Higdon, THE COYOTE UNIVERSE. I. PRECISION DETERMINATION OF THE NONLINEAR MATTER POWER SPECTRUM, *The Astrophysical Journal* **715**, 104 (2010).
- [16] K. Heitmann, E. Lawrence, J. Kwan, S. Habib, and D. Higdon, THE COYOTE UNIVERSE EXTENDED: PRECISION EMULATION OF THE MATTER POWER SPECTRUM, *The Astrophysical Journal* **780**, 111 (2013).
- [17] J. DeRose, R. H. Wechsler, J. L. Tinker, M. R. Becker, Y.-Y. Mao, T. McClintock, S. McLaughlin, E. Rozo, and Z. Zhai, The Aemulus Project. I. Numerical Simulations for Precision Cosmology, *The Astrophysical Journal* **875**, 69 (2019).
- [18] T. McClintock, E. Rozo, M. R. Becker, J. DeRose, Y.-Y. Mao, S. McLaughlin, J. L. Tinker, R. H. Wechsler, and Z. Zhai, The Aemulus Project. II. Emulating the Halo Mass Function, *The Astrophysical Journal* **872**, 53 (2019).
- [19] Z. Zhai, J. L. Tinker, M. R. Becker, J. DeRose, Y.-Y. Mao, T. McClintock, S. McLaughlin, E. Rozo, and R. H. Wechsler, The Aemulus Project. III. Emulation of the Galaxy Correlation Function, *The Astrophysical Journal* **874**, 95 (2019).
- [20] R. E. Smith and R. E. Angulo, Precision modelling of the matter power spectrum in a Planck-like Universe, *Monthly Notices of the Royal Astronomical Society* **486**, 1448 (2019).
- [21] T. Nishimichi, M. Takada, R. Takahashi, K. Osato, M. Shirasaki, T. Oogi, H. Miyatake, M. Oguri, R. Murata, Y. Kobayashi, and N. Yoshida, Dark Quest. I. Fast and Accurate Emulation of Halo Clustering Statistics and Its Application to Galaxy Clustering, *The Astrophysical Journal* **884**, 29 (2019).
- [22] D. Valcin, F. Villaescusa-Navarro, L. Verde, and A. Racanelli, BE-HAPPY: bias emulator for halo power spectrum including massive neutrinos, *Journal of Cosmology and Astroparticle Physics* **2019** (12), 057.
- [23] G. Aric o, R. E. Angulo, S. Contreras, L. Ondaro-Mallea, M. Pellejero-Iba nez, and M. Zennaro, The BACCO simulation project: a baryonification emulator with neural networks, *MNRAS* **506**, 4070 (2021), arXiv:2011.15018

- [astro-ph.CO].
- [24] F. Villaescusa-Navarro, C. Hahn, E. Massara, A. Banerjee, A. M. Delgado, D. K. Ramanah, T. Charnock, E. Giusarma, Y. Li, E. Allys, A. Brochard, C. Uhlemann, C.-T. Chiang, S. He, A. Pisani, A. Obuljen, Y. Feng, E. Castorina, G. Contardo, C. D. Kreisch, A. Nicola, J. Alsing, R. Scoccimarro, L. Verde, M. Viel, S. Ho, S. Mallat, B. Wandelt, and D. N. Spergel, *The Quijote Simulations*, *The Astrophysical Journal Supplement Series* **250**, 2 (2020), arXiv:1909.05273 [astro-ph.CO].
- [25] K. Heitmann, D. Bingham, E. Lawrence, S. Bergner, S. Habib, D. Higdon, A. Pope, R. Biswas, H. Finkel, N. Frontiere, and S. Bhattacharya, *THE MIRA-TITAN UNIVERSE: PRECISION PREDICTIONS FOR DARK ENERGY SURVEYS*, *The Astrophysical Journal* **820**, 108 (2016).
- [26] E. Lawrence, K. Heitmann, J. Kwan, A. Upadhye, D. Bingham, S. Habib, D. Higdon, A. Pope, H. Finkel, and N. Frontiere, *The Mira-Titan Universe. II. Matter Power Spectrum Emulation*, *The Astrophysical Journal* **847**, 50 (2017).
- [27] S. Bocquet, K. Heitmann, S. Habib, E. Lawrence, T. Uram, N. Frontiere, A. Pope, and H. Finkel, *The Mira-Titan Universe. III. Emulation of the Halo Mass Function*, *Astrophys. J.* **901**, 5 (2020), arXiv:2003.12116 [astro-ph.CO].
- [28] K. R. Moran, K. Heitmann, E. Lawrence, S. Habib, D. Bingham, A. Upadhye, J. Kwan, D. Higdon, and R. Payne, *The Mira-Titan Universe - IV. High-precision power spectrum emulation*, *MNRAS* **520**, 3443 (2023), arXiv:2207.12345 [astro-ph.CO].
- [29] J. Kwan, S. Saito, A. Leauthaud, K. Heitmann, S. Habib, N. Frontiere, H. Guo, S. Huang, A. Pope, and S. Rodríguez-Torres, *Galaxy Clustering in the Mira-Titan Universe. I. Emulators for the Redshift Space Galaxy Correlation Function and Galaxy-Galaxy Lensing*, *Astrophys. J.* **952**, 80 (2023), arXiv:2302.12379 [astro-ph.CO].
- [30] I. Sáez-Casares, Y. Rasera, T. R. G. Richardson, and P. S. Corasaniti, *The e-MANTIS emulator: Fast and accurate predictions of the halo mass function in $f(R)$ CDM and w CDM cosmologies*, *Astronomy & Astrophysics* **691**, A323 (2024), arXiv:2410.05226 [astro-ph.CO].
- [31] Euclid Collaboration, M. Knabenhans, and J. Stadel et al., *Euclid preparation: II. The EuclidEmulator – a tool to compute the cosmology dependence of the nonlinear matter power spectrum*, *Monthly Notices of the Royal Astronomical Society* **484**, 5509 (2019), <https://academic.oup.com/mnras/article-pdf/484/4/5509/27790453/stz197.pdf>.
- [32] Euclid Collaboration, M. Knabenhans, and J. Stadel et al., *Euclid preparation: IX. EuclidEmulator2 – power spectrum emulation with massive neutrinos and self-consistent dark energy perturbations*, *Monthly Notices of the Royal Astronomical Society* **505**, 2840 (2021).
- [33] Z. Chen, Y. Yu, J. Han, and Y. P. Jing, *CSST Cosmological Emulator I: Matter Power Spectrum Emulation with one percent accuracy*, arXiv e-prints, arXiv:2502.11160 (2025), arXiv:2502.11160 [astro-ph.CO].
- [34] Z. Chen and Y. Yu, *CSST Cosmological Emulator II: Generalized Accurate Halo Mass Function Emulation*, arXiv e-prints, arXiv:2506.09688 (2025), arXiv:2506.09688 [astro-ph.CO].
- [35] Y. Yang, S. Bird, and M.-F. Ho, *Ten-parameter simulation suite for cosmological emulation beyond Λ CDM*, *Phys. Rev. D* **111**, 083529 (2025), arXiv:2501.06296 [astro-ph.CO].
- [36] L. Cabayol-Garcia, J. Chaves-Montero, A. Font-Ribera, and C. Pedersen, *A neural network emulator for the Lyman- α forest 1D flux power spectrum*, *MNRAS* **525**, 3499 (2023), arXiv:2305.19064 [astro-ph.CO].
- [37] K. Diao and Y. Mao, *Multi-fidelity emulator for large-scale 21 cm lightcone images: a few-shot transfer learning approach with generative adversarial network*, arXiv e-prints, arXiv:2502.04246 (2025), arXiv:2502.04246 [astro-ph.IM].
- [38] DESI Collaboration, M. Abdul-Karim, and J. Aguilar et al., *DESI DR2 Results II: Measurements of Baryon Acoustic Oscillations and Cosmological Constraints*, arXiv e-prints, arXiv:2503.14738 (2025), arXiv:2503.14738 [astro-ph.CO].
- [39] DESI Collaboration, A. G. Adame, and J. Aguilar et al., *DESI 2024 VI: Cosmological Constraints from the Measurements of Baryon Acoustic Oscillations*, arXiv e-prints, arXiv:2404.03002 (2024), arXiv:2404.03002 [astro-ph.CO].
- [40] DES Collaboration, T. M. C. Abbott, and M. Acevedo et al., *Dark Energy Survey: implications for cosmological expansion models from the final DES Baryon Acoustic Oscillation and Supernova data*, arXiv e-prints, arXiv:2503.06712 (2025), arXiv:2503.06712 [astro-ph.CO].
- [41] M.-F. Ho, S. Bird, and C. R. Shelton, *Multifidelity emulation for the matter power spectrum using Gaussian processes*, *MNRAS* **509**, 2551 (2022), arXiv:2105.01081 [astro-ph.CO].
- [42] M.-F. Ho, S. Bird, M. A. Fernandez, and C. R. Shelton, *MF-Box: multifidelity and multiscale emulation for the matter power spectrum*, *MNRAS* **526**, 2903 (2023), arXiv:2306.03144 [astro-ph.CO].
- [43] Y. Yang, S. Bird, M.-F. Ho, and M. Qezlou, *Design and optimization of neural networks for multifidelity cosmological emulation*, arXiv e-prints (2025), submitted concurrently to arXiv.
- [44] A. G. Adame, J. Aguilar, S. Ahlen, S. Alam, and D. M. Alexander et al., *DESI 2024 VI: cosmological constraints from the measurements of baryon acoustic oscillations*, *Journal of Cosmology and Astroparticle Physics* **2025**, 021 (2025), arXiv:2404.03002 [astro-ph.CO].
- [45] Planck Collaboration, N. Aghanim, and Y. Akrami et al., *Planck 2018 results. VI. Cosmological parameters*, *Astronomy & Astrophysics* **641**, A6 (2020), arXiv:1807.06209 [astro-ph.CO].
- [46] Y. Feng, S. Bird, L. Anderson, A. Font-Ribera, and C. Pedersen, *MP-Gadget/MP-Gadget: A tag for getting a DOI* (2018).
- [47] W. R. M. Shan Ba and W. A. Brenneman, *Optimal Sliced Latin Hypercube Designs*, *Technometrics* **57**, 479 (2015), <https://doi.org/10.1080/00401706.2014.957867>.
- [48] M. Chevallier and D. Polarski, *Accelerating Universes with Scaling Dark Matter*, *International Journal of Modern Physics D* **10**, 213 (2001), arXiv:gr-qc/0009008 [gr-qc].
- [49] E. V. Linder, *Exploring the Expansion History of the Universe*, *Phys. Rev. Lett.* **90**, 091301 (2003), arXiv:astro-ph/0208512 [astro-ph].
- [50] Y. Ali-Haïmoud and S. Bird, *An efficient implementation of massive neutrinos in non-linear structure formation simulations*, *MNRAS* **428**, 3375 (2013), arXiv:1209.0461

- [astro-ph.CO].
- [51] S. Bird, Y. Ali-Haïmoud, Y. Feng, and J. Liu, An efficient and accurate hybrid method for simulating non-linear neutrino structure, *MNRAS* **481**, 1486 (2018), arXiv:1803.09854 [astro-ph.CO].
 - [52] J. Lesgourgues and S. Pastor, Massive neutrinos and cosmology, *Physics Reports* **429**, 307 (2006), arXiv:astro-ph/0603494 [astro-ph].
 - [53] V. F. Shvartsman, Density of relict particles with zero rest mass in the universe, *Pisma Zh. Eksp. Teor. Fiz.* **9**, 315 (1969).
 - [54] G. Steigman, D. N. Schramm, and J. E. Gunn, Cosmological Limits to the Number of Massive Leptons, *Phys. Lett. B* **66**, 202 (1977).
 - [55] Katrin Collaboration, M. Aker, D. Batzler, and A. Beglarian et al., Direct neutrino-mass measurement based on 259 days of KATRIN data, *Science* **388**, 180 (2025), arXiv:2406.13516 [nucl-ex].
 - [56] R. E. Angulo and A. Pontzen, Cosmological N-body simulations with suppressed variance, *MNRAS* **462**, L1 (2016), arXiv:1603.05253 [astro-ph.CO].
 - [57] DESI Collaboration, W. Elbers, A. Aviles, and H. E. Noriega et al., Constraints on Neutrino Physics from DESI DR2 BAO and DR1 Full Shape, arXiv e-prints , arXiv:2503.14744 (2025), arXiv:2503.14744 [astro-ph.CO].

Parameter Sensitivity

In Fig. 5, we show how the matter power spectrum varies with the cosmological parameters at $z = 0$ and $z = 2$. The reference cosmology is the same as that used in Ref. [35]. We see that large variations (up to $\sim 150\%$) in the matter power spectrum are supported by GokuNEmu around θ_{ref} . While the results for $z = 0$ are consistent with those in our previous work [35], we notice that the current predictions are more accurate and smoother. For instance, GokuEmu failed to accurately generate matter power spectra for w_a near the lower bound of its prior range (see panel 7 of Fig. 15 of Ref. [35]), while GokuNEmu successfully captures the dependence of the matter power spectrum on w_a throughout the prior range.

From the figure, we also find that the most sensitive k mode (denoted as k_s) at which the matter power spectrum varies with each of the parameters changes with redshift, typically shifting to higher k as redshift increases. The values of k_s has changed compared to those in Ref. [35], given that the current emulator is more accurate and has a wider range of k modes. For instance, k_s for Ω_m at $z = 0$ is now $\sim 10.99h/\text{Mpc}$ (upper limit of GokuNEmu's range), while it was $\sim 0.90h/\text{Mpc}$ in Ref. [35]. Another noticeable fact is that, for most of the parameters, the matter power spectrum is more sensitive to their changes at $z = 2$ than at 0 (thus wider fractional variations), except for n_s , w_0 , and w_a .

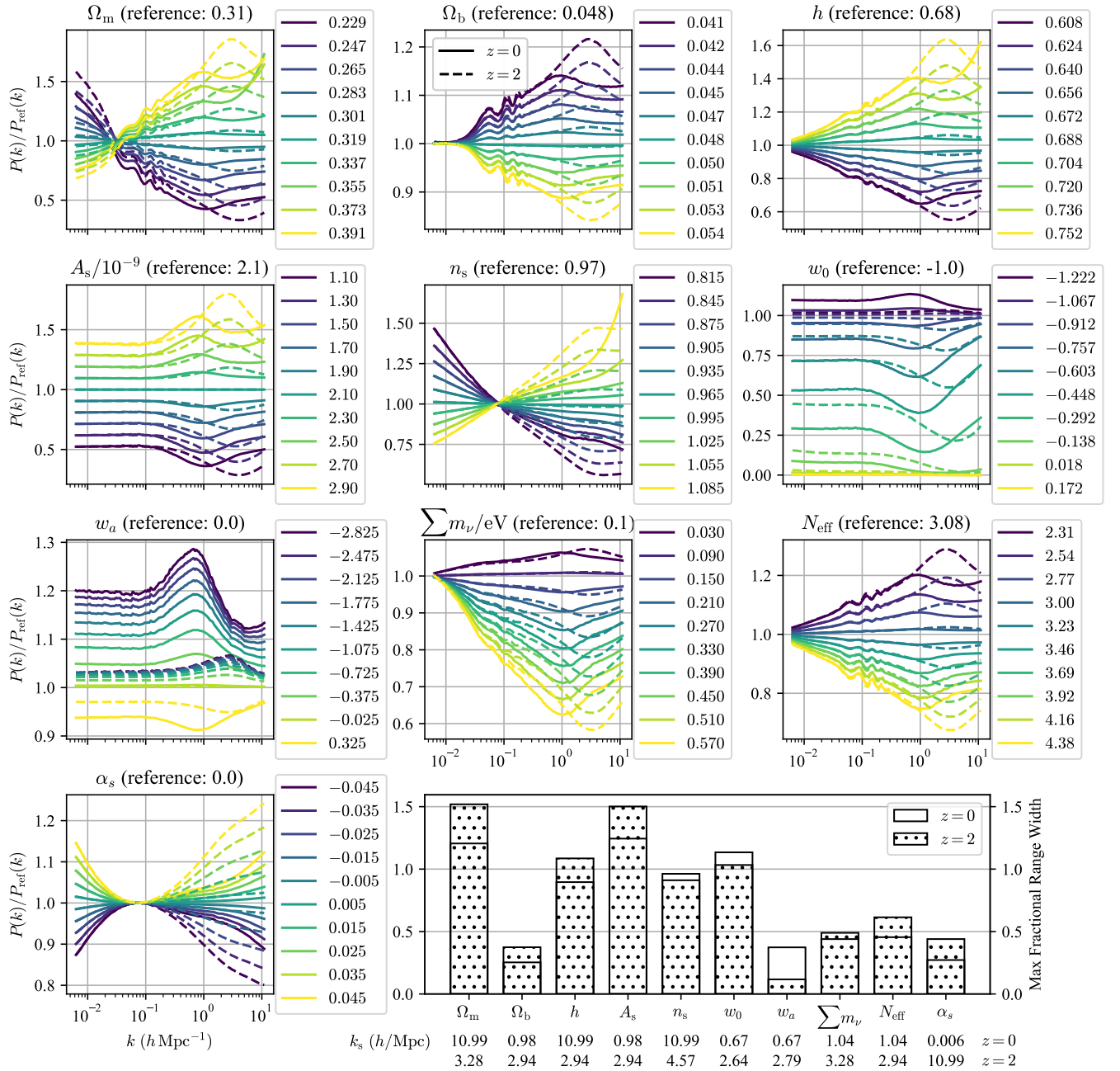


FIG. 5. Panels 1 to 10: variations in the matter power spectrum at $z = 0$ induced by each of 10 cosmological parameters, evaluated at the reference cosmology (defined in Ref. [35]). In each panel, one parameter is varied across 10 values, spanning from 5% to 95% of its prior range, while all other parameters are fixed at their reference values. The power spectra are normalized to the reference spectrum, with distinct colors indicating different parameter values. When we refer to panels 1 to 10, they are arranged sequentially from left to right and then top to bottom. Panel 11: the size of the fractional range of variation (difference between the largest and smallest power values across k modes) of the matter power spectrum, relative to the reference cosmology, is shown for each parameter. The scale at which this maximum range occurs is indicated below the corresponding parameter name for each redshift.